Hindawi
Shock and Vibration
Volume 2023, Article ID 2698650, 8 pages
https://doi.org/10.1155/2023/2698650

Research Article

Improving Critical Frequency of the Electrothermal V-Shaped Actuator Using the Particle Swarm Optimization Algorithm

Phuc Hong Pham,[1] **Phuc Truong Duc**,[1] **Kien Trung Hoang**,[2] **and Ngoc-Tam Bui**[3]

[1]*Hanoi University of Science and Technology, Hanoi, Vietnam*
[2]*Le Quy Don Technical University, Hanoi, Vietnam*
[3]*Shibaura Institute of Technology, Tokyo, Japan*

Correspondence should be addressed to Kien Trung Hoang; kienhoangtrung87@gmail.com

Received 8 June 2023; Revised 2 November 2023; Accepted 7 November 2023; Published 1 December 2023

Academic Editor: Rodrigo Nicoletti

This paper presents a thermal transfer model and optimization of a V-beam dimension to improve the critical frequency f_C (i.e., expanding the effective working frequency range) of an electrothermal V-shaped actuator (EVA). The obtained results are based on applying the finite difference model, a method for calculating the critical frequency, as well as conditions to ensure the mechanical stability and thermal safety of EVA. The influence of beam dimensions (i.e., length L, width w, and incline angle θ of the beam) on the variation of critical frequency f_C is investigated and evaluated. Moreover, the particle swarm optimization (PSO) algorithm is used to figure out the optimal beam dimensions aiming to increase the critical frequency while satisfying conditions such as mechanical stability, thermal safety, and suitable displacement of EVA. With the optimal dimensions of V-beam ($L = 679\,\mu$m, $w = 4\,\mu$m, and $\theta = 1.8^\circ$), the critical frequency of the V-shaped actuator can be achieved up to 136.22 Hz at a voltage of 32 V (average increment of f_C is 33.1% with the driving voltage changing from 16 V to 32 V) in comparison with the nonoptimal structure (f_C is only 102.34 Hz at 32 V).

1. Introduction

The electrothermal V-shaped actuator (EVA) is a type of MEMS (microelectromechanical systems) device that plays a role of driving microsystems such as microgripper [1], micromotor [2], nanomaterial testing equipment [3], and thermal safety equipment [4]. This actuator works on the principle of converting electrical energy into heat and thermal expansion. The outstanding advantages of EVA are large output force, low conduction voltage, and simple structure. However, the drawback of the V-shaped actuator is the long response time due to thermal hysteresis. Recently, there have been many publications on EVA related to improvement/optimization issues such as developing accurate heat transfer models [5], improving structure [6], working frequency [7], or geometric optimization [8].

Studies on mathematical methods to describe the heat transfer process of EVA have been a main topic in the last decade. The analytical methods have been used to model steady-state heat transfer [9], or unstable heat transfer [10]. The finite difference heat transfer model was used to determine the change and distribution of temperature on the beam with time as shown in references [5, 11]. These are two methods that are used quite commonly. In addition, there are some others such as equivalent circuits [12] and the nodal point method [13]. In these models, the finite difference model is simpler than the analytical method, but the nonlinearity of the material can be taken into account. In order to increase the displacement of EVA, some new structures have been proposed such as using the lever arm principle [14] or combining with the U-shaped structure [15].

Determining the effective working frequency range of EVA is important to design and apply the EVA in microelectromechanical systems. Regarding the thermal response of the actuator, the time constant factor (time for the temperature to reach a steady state) has been proposed in reference [16]. However, this quantity is determined by solving the approximation and taking the approximate value while treating

the material parameters as constants. The effective working frequency range determined through the threshold frequency has been suggested by the authors in reference [7]. The value of the critical frequency has been determined based on the finite difference heat transfer model. Research on dimension optimization of EVA has also been interested, in which GA (genetic algorithm) and PSO (particle swarm optimization) have been, respectively, applied for optimizing dimensions to reduce stress concentration [8] and increase thermal efficiency [17].

These studies have made important contributions in proposing appropriate and efficient mathematics models, proposing reasonable structures to increase displacement, determining thermal response time and frequency, or introducing EVA's optimal size. However, the influence of the dimension parameters on the critical frequency value and increasing the effective working frequency range of EVA while ensuring mechanical stability as well as safe working requirements has not been mentioned in detail.

This paper describes the heat transfer process on V-beams by using a finite difference electrothermal-mechanical model, which takes into account the change of thermal conduction coefficient, resistivity, and thermal expansion coefficient with temperature. Accordingly, a theoretical calculation is established to investigate the dependence of the critical working frequency on the beam dimensions. The PSO algorithm is also applied to determine the optimal dimensions for improving the critical frequency, that is, for not only obtaining suitable displacement but also for satisfying the axial stability of the V-beam and thermal safety of EVA.

2. Configuration and the Heat Transfer Model

2.1. Configuration and Operation. The structure of a typical electrothermal V-shaped actuator is shown in Figure 1.

The actuator consists of three main parts: the central shuttle (1); V-shaped beams (2); and fixed electrodes (3). The shuttle (1) at the center is suspended by pairs of V-shaped beams (2), and the other ends of the beams are attached to two fixed electrodes (3). The main dimensions and geometric parameters include the following: L, w, and h are the length, width, and thickness of the beam, respectively, θ is the incline angle of the beam in the X-direction, g_a is the air gap between the structural layer and the substrate (i.e., the SiO_2 buffer layer of the silicon on insulator: SOI wafer), and n is the pair number of V-beam. When voltage is applied on two fixed electrodes (3), the current conducting through the V-beams generates heat and expansion, causes a combined force, and pushes the shuttle (1) moving in the Y-direction. If the voltage goes to zero, the temperature on the beams decreases and the beams will shrink and pull the shuttle back.

2.2. Heat Transfer Model and Thermal Expansion Force. Heat transfer in a thin beam is a very complicated process and is influenced by a few factors such as environment, microactuator structure, and materials. To facilitate the establishment of mathematical models, the following assumptions are used: neglect heat loss from the shuttle, ignore

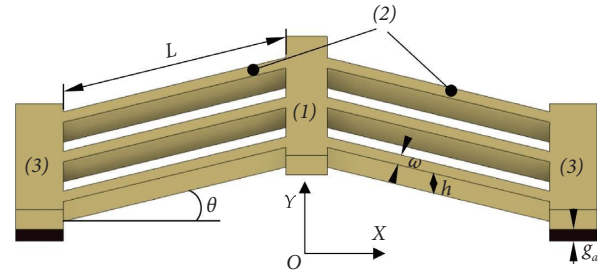

Figure 1: Configuration of the EVA.

radiation and convection in the air, heat transfer in the beam is unidirectional and along the beam axis, and heat is transferred from electrodes to substrate and from the substrate to air is ideal. According to reference [18], the finite difference heat transfer equation for the i^{th} segment of the thin beam at time stage $j+1$ has the following form:

$$T_i^{j+1} = \frac{k}{C_p d}\frac{\Delta t}{\Delta x^2}T_{i-1}^j + \left(1 - 2\frac{k}{C_p d}\frac{\Delta t}{\Delta x^2} - \frac{k_a S}{h g_a}\frac{\Delta t}{C_p \cdot d}\right)T_i^j + \frac{k}{C_p d}\frac{\Delta t}{\Delta x^2}T_{i+1}^j + \frac{k_a S}{h g_a}\frac{\Delta t}{C_p \cdot d}T_0 + \frac{U^2}{4\rho L^2}\frac{\Delta t}{C_p \cdot d}, \tag{1}$$

where k and k_a are the thermal conductivity of silicon and air, respectively, T_i^j is the temperature of the i^{th} beam segment at time stage j, T_0 is the room temperature, $S = S(h/w)$ is the shape factor of the beam cross-section depending on the (h/w) ratio, C_p, d, and ρ are the specific heat, density, and resistivity of silicon, respectively, U is the driving voltage, and Δt is the time increment.

On the total length of $2L$, a V-beam is divided into m similar segments with a length of Δx and corresponding to a system of m equations as shown in equation (1). With the boundary condition: $T_{(i=1)} = T_{(i=m)} = T_0$ and the initial condition: $T_{(j=1)} = T_0$, the temperature distribution on the beam at different times will be completely determined by solving the system of m equations mentioned above.

The thermal expansion of a beam is calculated according to the formula as follows:

$$\Delta L = \frac{1}{2}\sum_{i=1}^{m} \alpha (T_i - T_0)\Delta x, \tag{2}$$

where α is the thermal expansion coefficient of silicon material.

Referring from our previous publication [18], the total thermal expansion force acting on the shuttle in Y-direction is calculated as

$$F = 2n\mathrm{AE}\frac{\Delta L}{L}\sin\theta, \tag{3}$$

where F_b is a thermal expansion force along the single beam (detailed in Section 3.2), $A = h \cdot w$ is the area of the beam cross-section, $E = 1.69 \times 10^5$ (MPa) is Young's modulus of silicon, and n is the number of beam pairs.

2.3. The Displacement of the EVA. K is the equivalent stiffness of the V-beam system which is calculated as follows [18]:

$$K = \frac{2nE\left(12I\cos^2\theta + \mathrm{AL}^2\sin^2\theta\right)}{L^3}, \quad (4)$$

where $I = h \cdot w^3/12$ is the inertia moment of the beam's cross-sectional area.

The static displacement Y_m of the shuttle (i.e., of a V-shaped actuator) is calculated as follows:

$$Y_m = \frac{F}{K}. \quad (5)$$

From equations (3)–(5), we have

$$Y_m = \frac{\mathrm{AL}^2}{12I\cos^2\theta + AL^2\sin^2\theta}\Delta L\sin\theta. \quad (6)$$

We can see that the displacement Y_m depends on the thermal expansion length ΔL and the dimension parameters of the beam such as the beam length L, the beam width w, and the incline angle θ.

3. Critical Frequency, Mechanical Stability, and Thermal Safety Conditions

3.1. Critical Frequency f_C. Considering a square pulse voltage with period T_U used to drive the EVA, the power supply time t_{ON} is equal to the power off time t_{OFF} in one cycle ($t_{\mathrm{ON}} = t_{\mathrm{OFF}} = T_U/2$). The critical frequency f_C in this case is defined as the maximum frequency value of the driving voltage that satisfies the following condition: the relative displacement reduction of the actuator is not less than the allowable value $\delta\%$ when comparing between instantaneous displacement Y and the maximum static displacement $Y_{\max}$. The critical frequency f_C is calculated as follows:

$$\begin{aligned} f_C &= \frac{1}{T_C} \\ &= \frac{1}{2t_C}, \end{aligned} \quad (7)$$

where T_C is the critical period and t_C is the critical power supply time in a cycle satisfying the condition as follows:

$$\frac{Y(t_C)}{Y_{\max}} = \left(1 - \frac{\delta_{\%}}{100}\right). \quad (8)$$

$Y(t_C)$ and $Y_{\max}$ are calculated by equation (6), while $Y_{\max} = Y(t \longrightarrow \infty)$ is combined with equation (2). So, we have

$$\begin{aligned} \frac{\Delta L(t_C)}{\Delta L_{\max}} &= \left(1 - \frac{\delta_{\%}}{100}\right) \text{or: } \frac{\sum_{i=1}^{m}\left(T_i^{t_C} - T_0\right)}{\sum_{i=1}^{m}\left(T_i^{t\longrightarrow\infty} - T_0\right)} \\ &= \left(1 - \frac{\delta_{\%}}{100}\right). \end{aligned} \quad (9)$$

When the allowable displacement reduction $\delta\%$ is given, the critical frequency depends on the beam dimension parameters (i.e., L, w, and θ) because the temperature distribution on the V-beam is also dependent on these parameters as shown in equation (1) through the shape factor $S(h/w)$ and the length of the beam element $\Delta x = (2L/m - 1)$.

3.2. Mechanical Stability and Thermal Safety Condition. If the actuator is working without load or external force, the displacement of the shuttle corresponds to the thermal expansion of the beam and can be computed by formula (6). At this state, the internal reaction force of a single beam N_b depends on the total value of the elastic force F_e. When the load P_c is applied on the top of the shuttle, the actuator will move in the Y-direction and will only stop if the thermal expansion force F_b, the total elastic force of the beam system F_e, and the load P_c are balanced (see, Figure 2). At the same time, a larger internal force N_b will appear along the beam because the actual elongation of the beam is less than the thermal expansion ΔL (i.e., the beam is being compressed longitudinally). If the internal force N_b is greater than the critical force P_{cr} on each beam, axial instability or beam-buckling phenomenon will occur and will reduce the bearing capacity of the actuator. To avoid the beam-buckling phenomenon, we need the condition: $N_b \le P_{cr}$.

In this case, formulas of N_b and P_{cr} can be referred from reference [18], and the axial stability condition of the beam is determined as follows:

$$\left(1 - \frac{\left(\mathrm{AL}^2 - 12I\right)\sin^2\theta\cos^2\theta}{\mathrm{AL}^2\sin^2\theta + 12I\cos^2\theta}\right)\mathrm{AE}\frac{\Delta L_{\max}}{L} \le \frac{4\pi^2\mathrm{EI}}{L^2}. \quad (10)$$

At a high temperature of the V-beam, some silicon material properties will change and reduce the plastic deformation strength. Overheating may occur and cause failure of the beams of the actuator if the beam temperature approaches the melting point of silicon (i.e., about 1414°C) [19]. Here, we call a "critical temperature" T_{cr} which is the temperature at which silicon begins to plasticize ($T_{\mathrm{cr}} \approx 1200$°C) as mentioned in reference [20]. The conditions to ensure thermal safety for a V-shaped actuator can be expressed as follows:

$$T_{\max} \le T_{cr} = 1200\text{°C}, \quad (11)$$

where $T_{\max}$ is the maximum temperature on the V-beam when reaching the thermal steady state.

4. Effect of Beam Dimension on Critical Frequency and Optimal Dimension of V-Beam

4.1. Effect of Beam Dimension on Critical Frequency of EVA. Similar to previous our work [18, 21], the V-shaped actuator has been fabricated by using SOI (silicon on insulator) wafer with 3 layers: the structure layer of 30 μm (i.e. the thickness $h = 30\,\mu$m

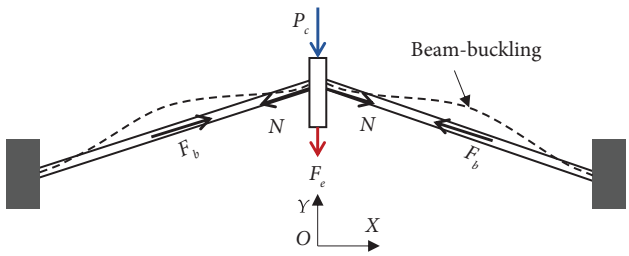

Figure 2: Forces acting on the EVA structure.

and cannot be changed), the SiO_2 buffer layer of 4 μm and the substrate of 450 μm. The material properties and parameters of the silicon device layer are given in Tables 1 and 2.

To validate the theoretical critical frequency *fc* calculated by equations (7) and (9), the 3D finite element model of the V-shaped beam (the dimensions, material properties, and ambient are given in Tables 1 and 2) was established by ANSYS Workbench 15. The model is meshed with a body size of 10 micrometers in both electric and transient thermal to simulate the nonlinear temperature on the V-shaped beam. The distribution of temperature along the V-beam at the voltage of 20 V and 25 V is shown in Figure 3, and the change of temperature in a time period is indicated in Figure 4.

According to Figure 4, the change of temperature on the V-beam calculated by equation (1) and the simulation is quite similar. The difference in steady-state temperature between the two ways is insignificant (approximately 4.3%). The time t_C to reach the steady state calculated by formula (9) and simulation is 0.0080 s and 0.0085 s, respectively (relative error is 5.88%). Thus, the results calculated according to the mathematical model proposed above when compared with the simulation are acceptable. Here, the tolerance can be explained as the heat transfer from the shuttle to the substrate is ignored while calculating.

In this case, we choose an allowable displacement reduction of $\delta\% = 1\%$. By solving equations (8) and (9), the relations between the critical frequency f_C, beam length L, and beam width w at a driving voltage of 30 V have been found and displayed in Figures 5 and 6, respectively.

From the graph in Figures 5 and 6, we can see that the value of critical frequency will decrease while increasing beam length L or beam width w. When the beam width changes from 4 μm to 8 μm, the value of frequency f_C will decrease significantly. As an example, at a beam length L = 600 μm and beam width gets a value of 4 μm and 8 μm, the critical frequency deviation is 51 Hz (i.e. reducing about 36.4% as shown in Figure 5). Similarly, if the beam length increases from 400 μm to 800 μm correspondence to beam width$w = 4$ μm, the critical frequency will reduce by about 21.5 Hz (frequency deviation is approximately 14.2% as shown inFigure 6).

Hence, in order to increase the critical frequency of the V-shaped actuator, one of the options suggested are as follows: (i) reducing the beam length L (low effect), (ii) reducing the beam width w (high effect), and (iii) reducing both beam length and width. However, changing beam dimensions may affect temperature allocation on the V-beam and cause some drawbacks such as overheating, axial instability, or loss of displacement. In order to figure out the best dimensions of V-beam not only for getting a higher critical frequency but also for satisfying save conditions such as mechanical stability and thermal safety, we propose to use a particle swarm optimization (PSO) algorithm as detailed in the next section.

4.2. Calculating the Dimension of V-Beam by Using a Particle Swarm Optimization (PSO) Algorithm. The PSO (particle swarm optimization) algorithm was first presented in 1995 by the authors in reference [22]. This algorithm offers several advantages over other optimization techniques such as being relatively simple, less coding, and efficient with many composite problems. Therefore, it will be used to obtain the optimal geometry dimensions of the V-beam. The mathematical form of the PSO algorithm can be written as follows [23]:

$$V_{j+1}^k = W_j V_j^k + C_1 r_1 \left(P_{\text{Best}}^k - X_j^k\right) + C_2 r_2 \left(G_{\text{Best}} - X_j^k\right),$$
$$X_{j+1}^k = X_j^k + V_{j+1}^k, \tag{12}$$

where X_j^k and V_j^k are the location and rate of particle k at the iteration j^{th}, W_j is the inertia factor, C_1 and C_2 are the particle and "social" effect coefficients, respectively, r_1 and r_2 are the numbers selected randomly in the range of [0, 1], P_{Best}^k is the best location of particle k, and G_{Best} is the best location of the swarm.

The method to solve the problem of finding the optimal dimension of EVA's beams by using PSO can be described specifically as follows.

We need to find the maximum value of the objective function $f_C = f(L, w, \text{and } \theta)$ calculated by equations (7) and (9) at voltages from 26 V to 30 V. The set of beam dimension (L, w, and θ) is limited due to the requirement of SOI-MEMS fabrication technology as follows: $\{400\,\mu\text{m} \le L \le 800\,\mu\text{m}\}$, $\{4\,\mu\text{m} \le w \le 10\,\mu\text{m}\}$, and $\{1^\circ \le \theta \le 3^\circ\}$. Additionally, it also satisfies constraints of boundary conditions at the same time.

The thermal safety condition inferred from condition (11) is as follows:

$$g_1 = T_{\max} - 1200^\circ\text{C} \le 0. \tag{13}$$

The axial stability of the V-beam from equation (10) is as follows:

$$g_2 = \left(1 - \frac{\left(\text{AL}^2 - 12I\right)\sin^2\theta\cos^2\theta}{\text{AL}^2\sin^2\theta + 12I\cos^2\theta}\right)\text{AE}\frac{\Delta L_{\max}}{L} - \frac{4\pi^2 EI}{L^2} \le 0. \tag{14}$$

According to displacement condition: $Y_{\max} \ge Y^*$, we have the third constrain as follows:

$$g_3 = Y^* - Y_{\max} \le 0, \tag{15}$$

where $Y^* \approx 64\,\mu$m is a theoretical displacement of EVA at $U = 30$ V corresponding to nonoptimal beam dimension (i.e., $L = 750\,\mu$m, $w = 6\,\mu$m, and $\theta = 2^\circ$) which has been designed and fabricated perfectly in [21].

Table 1: Material properties of silicon.

d (kg/μm^3)	E (MPa)	k_a (pW/μm·K)	C_p (pJ/kg·K)	ρ_0 (TΩ.μm)	λ (1/K)
2330×10^{-18}	169×10^{3}	2.57×10^{4}	7.12×10^{14}	230×10^{-12}	1.250×10^{-3}

Table 2: Material parameters change with temperature [19].

T (K)	300	400	500	600	700	800	900	1000	1100	1200	1300
k (10^{12}pW/μm·K)	1.56	1.05	0.80	0.64	0.52	0.43	0.36	0.31	0.28	0.26	0.25
α (10^{-8} 1/K)	262	325	361	384	402	415	418	426	432	438	444

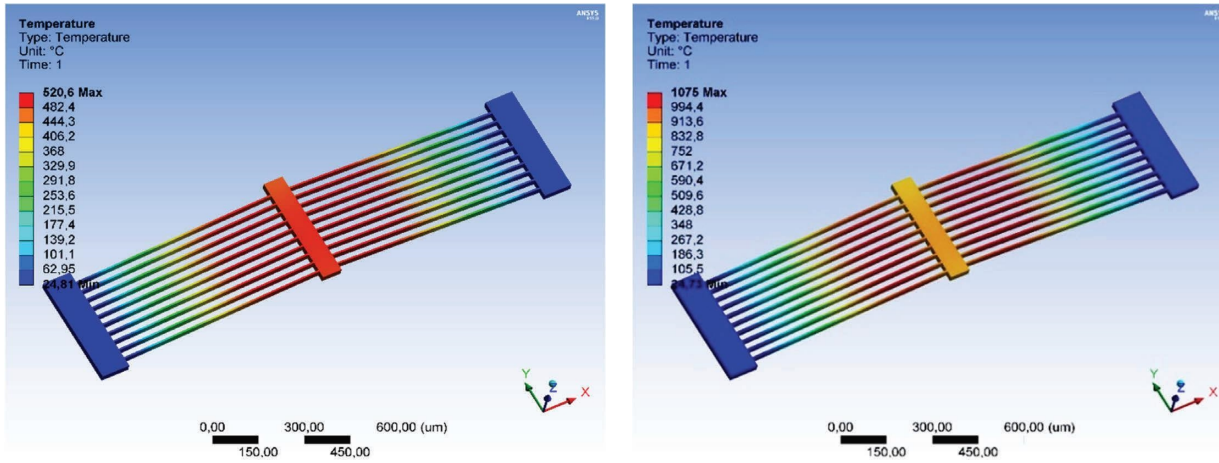

(a) (b)

Figure 3: The distribution of temperature along the V-beam at $U = 20$ V (a) and $U = 25$ V (b).

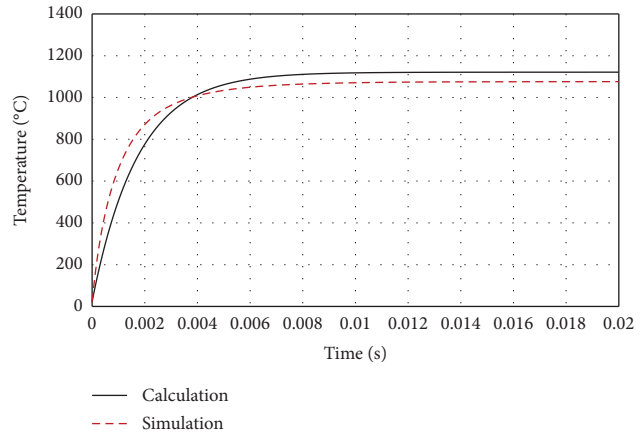

Figure 4: Comparison of the temperature-changing between simulation and calculation.

The optimal beam dimensions are determined by the PSO algorithm and solved by using MATLAB at some voltage values ranging between 26 V and 34 V. When comparing with nonoptimal structure, most of the optimal dimension sets give a higher critical frequency as listed in Table 3.

The optimal results clearly show that the critical frequency f_C is proportional to the driving voltage in the range from 26 V to 32 V and gets a maximum value of 136.22 Hz at $U = 32$ V. Beyond this range of voltage, the optimal critical frequency tends to decrease. The calculation results in Table 3 also clarify that the frequency f_C reaches a maximal value of 136.22 Hz at a voltage of 32 V with optimal beam dimension set ($L = 679\,\mu$m, $w = 4\,\mu$m, and $\theta = 1.8^\circ$). Besides, the frequency $f_C = 135.63$ Hz and maximum displacement $Y_m = 70.83\,\mu$m can be obtained at a voltage of 34 V with other beam dimension sets ($L = 722\,\mu$m, $w = 4\,\mu$m, and $\theta = 1.8^\circ$).

The critical frequencies and displacements of the EVA corresponding to two optimal dimension sets as mentioned above will be compared with the frequency and displacement of nonoptimal beam dimension (i.e., $L = 750\,\mu$m, $w = 6\,\mu$m, and $\theta = 2^\circ$) as in Figure 7. Here, the driving voltage changes from 16 V to 32 V.

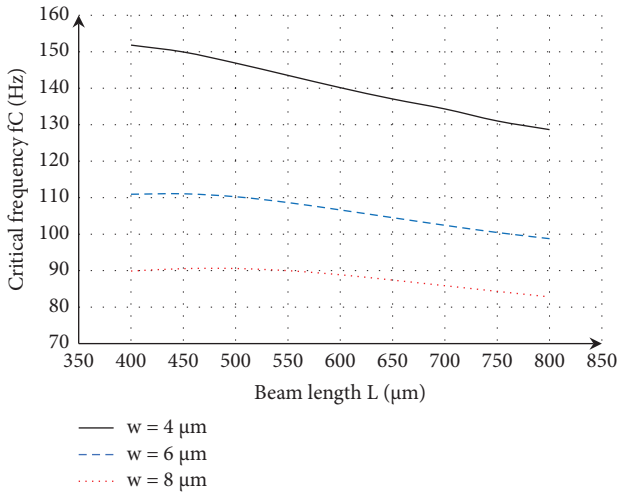

Figure 5: Relation between f_C and beam length L.

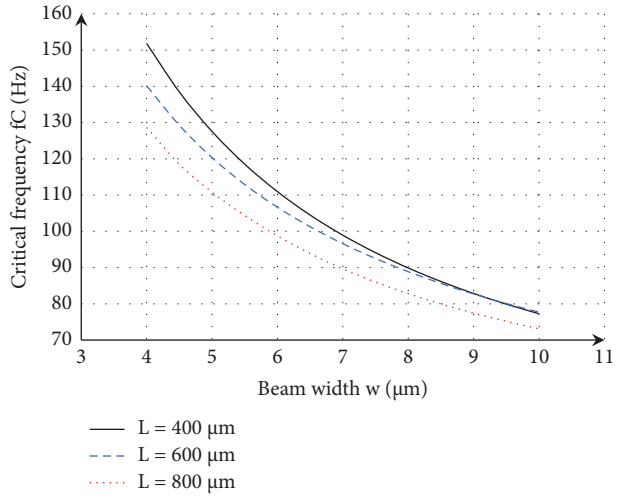

Figure 6: Relation between f_C and beam width w.

Table 3: Optimal beam dimensions and critical frequencies at various driving voltages.

U (V)	Optimal beam dimensions			$f_{C\text{-opt.}}$ (Hz)	$f_{C\text{-nonopt.}}$ (Hz)	Y_m (μm)
	L (μm)	w (μm)	θ (°)			
26	742	6.4	1.5	92.35	97.5	64.18
28	795	4.2	1.4	119.84	99.3	63.84
30	650	4	1.7	135.87	100.46	62.77
32	679	4	1.8	136.22	102.34	65.38
34	722	4	1.8	135.63	103.73	70.83

From the graph in Figure 7, it is clear that the EVA's beam dimension set determined by the PSO algorithm will give a much better critical frequency than the frequency of the nonoptimal dimension set. Here, the critical frequency increases by about 33.88 Hz (33.1%) and 29.3 Hz (28.2%) in proportion to the optimal dimension set at 32 V and 34 V as mentioned above, when considering the various voltages changing from 16 V to 32 V. When applying a voltage of

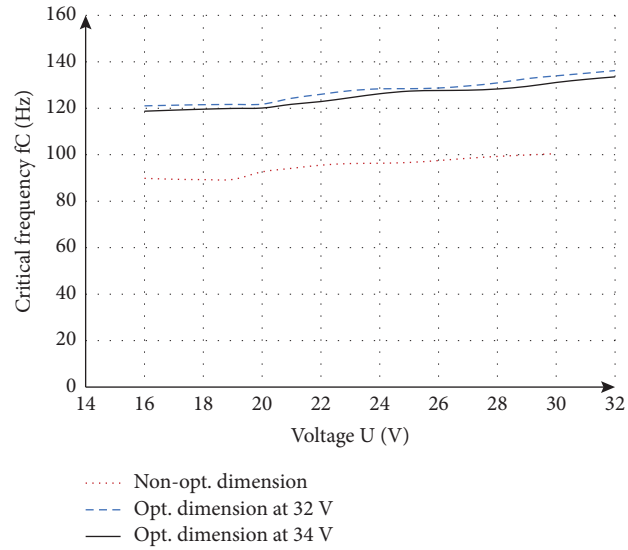

Figure 7: The comparison of critical frequency values.

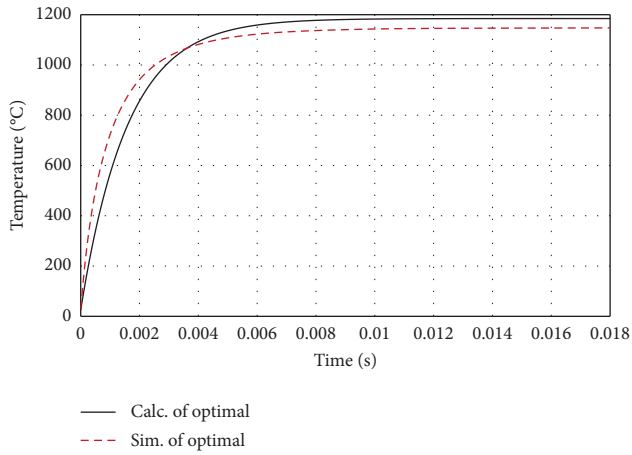

Figure 8: The changing temperature of the optimal V-beam at 32 V.

34 V, the maximum temperature of optimal V-beam ($L = 679\,\mu$m, $w = 4\,\mu$m, and $\theta = 1.8°$) is over critical temperature mentioned in (12). Thus, the calculation at 34 V is unused and neglected.

To verify the optimal calculation results, the V-shaped actuator with the optimal dimension set at 32 V (i.e., $L_t = 679\,\mu$m, $w_t = 4\,\mu$m, and $\theta_t = 1.8°$) was simulated. The results of the variation of beam temperature with time calculated according to both models are shown in Figure 8. The deviation in both the temperature at the steady state and the time to reach the steady state between the two methods is only 3.2% and 9%, respectively. The result reconfirms the advantage of the optimal model.

Therefore, these sets of optimal dimensions help to expand the working frequency range of EVA while still satisfying the conditions of thermal safety in reference (13), mechanical stability in reference (14), and minimum displacement in reference (15) as mentioned above. In particular, the optimal dimension set of EVA at $U = 32$ V

($L = 679\,\mu$m, $w = 4\,\mu$m, and $\theta = 1.8^{\circ}$) gives the maximum critical frequency (i.e., largest effective frequency range) and it can be applied in the design and calculation of thermal-based microdevices using V-shaped actuators such as micromotor, microgripper, or microconveyance system.

5. Conclusion

This study used a finite difference heat transfer model applied for a V-shaped actuator structure to determine more accurately the change and distribution of temperature on the V-beam. Besides, the conditions of thermal safety and axial stability of the V-beam have been carefully proposed and investigated. The dependence of the critical frequency on beam geometry dimensions was also studied. Furthermore, the PSO algorithm is applied to compute the optimal geometry dimensions of the V-beam to achieve the best critical frequency while satisfying the conditions of thermal safety, mechanical stability, and suitable displacement. A set of optimal beam dimension ($L_t = 679\,\mu$m, $w_t = 4\,\mu$m, and $\theta_t = 1.8^{\circ}$) working with the square wave voltage changes from 16 V to 32 V thereby expanding to an effective working frequency range. In other words, it provides the critical frequency f_C of up to 136.22 Hz (increasing about 33.1% in comparison with a set of nonoptimal dimensions as mentioned in [21]). The accuracy of the proposed model and the optimal result are improved as discussed at the end of Section 4.2.

These results may be a valuable suggestion/instruction to design and optimize the MEMS devices driven by the V-shaped actuator structure, which tend to improve the working capability and safety of the system as well as extend their lifetime.

Data Availability

No data were used to support the study.

Conflicts of Interest

The authors declare that they have no conflicts of interest.

Acknowledgments

This research was supported by the Centennial SIT Action for the 100th anniversary of the Shibaura Institute of Technology to enter the top ten Asian Institute of Technology.

References

[1] P. Shivhare, G. Uma, and M. Umapathy, "Design enhancement of a chevron electrothermally actuated microgripper for improved gripping performance," *Microsystem Technologies*, vol. 22, no. 11, pp. 2623–2631, 2016.

[2] A. Geisberger, D. Kadylak, and M. Ellis, "A silicon electrothermal rotational micro motor measuring one cubic millimeter," *Journal of Micromechanics and Microengineering*, vol. 16, no. 10, pp. 1943–1950, 2006.

[3] Y. Zhu, A. Corigliano, and H. D. Espinosa, "A thermal actuator for nanoscale in situ microscopy testing: design and characterization," *Journal of Micromechanics and Microengineering*, vol. 16, no. 2, pp. 242–253, 2006.

[4] T. Hu, Y. Zhao, X. Li, Y. Zhao, and Y. Bai, "Integration design of MEMS electro-thermal safety-and-arming devices," *Microsystem Technologies*, vol. 23, no. 4, pp. 953–958, 2017.

[5] C. D. Lott, T. W. McLain, J. N. Harb, and L. L. Howell, "Modeling the thermal behavior of a surface-micromachined linear-displacement thermomechanical microactuator," *Sensors and Actuators A: Physical*, vol. 101, no. 1-2, pp. 239–250, 2002.

[6] X. Shen and X. Chen, "Mechanical performance of a cascaded V-shaped electrothermal actuator," *International Journal of Advanced Robotic Systems*, vol. 10, no. 11, p. 379, 2013.

[7] D. T. Nguyen, K. T. Hoang, and P. H. Pham, "Heat transfer model and critical driving frequency of electrothermal V-shaped actuators," *Advances in Engineering Research and Application*, vol. 104, pp. 394–405, 2020.

[8] M. S. Suen, J. C. Hsieh, K. C. Liu, and D. T. W. Lin, "Optimal design of the electrothermal V-beam microactuator based on GA for stress concentration analysis," *Lecture Notes in Engineering and Computer Science*, vol. 2, pp. 1264–1268, 2011.

[9] Z. Zhang, W. Zhang, Q. Wu, Y. Yu, X. Liu, and X. Zhang, "Closed-form modelling and design analysis of V- and Z-shaped electrothermal microactuators," *Journal of Micromechanics and Microengineering*, vol. 27, no. 1, Article ID 015023, 2017.

[10] Z. Zhang, Y. Yu, X. Liu, and X. Zhang, "Dynamic modelling and analysis of V- and Z-shaped electrothermal microactuators," *Microsystem Technologies*, vol. 23, no. 8, pp. 3775–3789, 2017.

[11] T. Shan, X. Qi, L. Cui, and X. Zhou, "Thermal behavior modeling and characteristics analysis of electrothermal microactuators," *Microsystem Technologies*, vol. 23, no. 7, pp. 2629–2640, 2017.

[12] B. López-Walle, M. Gauthier, and N. Chaillet, "Dynamic modelling for thermal micro-actuators using thermal networks," *International Journal of Thermal Sciences*, vol. 49, no. 11, pp. 2108–2116, 2010.

[13] R. G. Li, Q. A. Huang, and W. H. Li, "A nodal analysis method for simulating the behavior of electrothermal microactuators," *Microsystem Technologies*, vol. 14, no. 1, pp. 119–129, 2007.

[14] Y.-L. Zhao, T.-J. Hu, X.-Y. Li, Z.-D. Jiang, W. Ren, and Y.-W. Bai, "Design and characterization of a large displacement electro-thermal actuator for a new kind of safety-and-arming device," *Energy Harvesting and Systems*, vol. 2, no. 3-4, pp. 143–148, 2015.

[15] J. J. Khazaai, M. Haris, M. Khir, H. Qu, and J. Slicker, "Design and fabrication of a low power electro-thermal V-shape actuator with large displacement," *NSTI-Nanotech*, vol. 2, pp. 681–684, 2010.

[16] R. Hickey, D. Sameoto, T. Hubbard, and M. Kujath, "Time and frequency response of two-arm micromachined thermal actuators," *Journal of Micromechanics and Microengineering*, vol. 13, no. 1, pp. 40–46, 2003.

[17] S. E. Osman and M. Zarog, "Optimized V-shaped beam micro-electrothermal actuator using particle swarm optimization (PSO) technique," *Micro and Nanosystems*, vol. 11, no. 1, pp. 62–67, 2019.

[18] K. T. Hoang, D. T. Nguyen, and P. H. Pham, "Impact of design parameters on working stability of the electrothermal V-shaped actuator," *Microsystem Technologies*, vol. 26, no. 5, pp. 1479–1487, 2020.

[19] R. Hull, *Properties of Crystalline Silicon*, INSPEC, Uttar Pradesh, India, 1999.

[20] K. T. Hoang and P. H. Pham, "Safe working condition and optimal dimension of the electrothermal V-shaped actuator," *Microsystem Technologies*, vol. 28, no. 7, pp. 1673–1685, 2022.

[21] D. T. Nguyen, K. T. Hoang, and P. H. Pham, "Larger displacement of silicon electrothermal V-shaped actuator using surface sputtering process," *Microsystem Technologies*, vol. 27, no. 5, pp. 1985–1991, 2021.

[22] J. Kennedy and R. Eberhart, "Particle swarm optimization," *Proceedings of ICNN'95- International Conference on Neural Networks*, vol. 4, pp. 1942–1948, 1995.

[23] Y. Shi and R. Eberhart, "A modified particle swarm optimizer," in *Proceedings of the 1998 IEEE International Conference on Evolutionary Computation Proceedings IEEE World Congress on Computational Intelligence (Cat. No.98TH8360)*, pp. 69–73, Anchorage, AK, USA, June 1998.